Available online at www.sciencedirect.com

ScienceDirect

IFAC Papers Online CONFERENCE PAPER ARCHIVE

IFAC PapersOnLine 59-9 (2025) 43–48

Learning-based Detection of Fault Type and Location in Electrical Distribution Networks ⋆

Sajjad Miralizadeh Jalalat *,** **Alberto Cavallo** *
Antonio Russo *** **Francesco Tucci** *,**

* *Dipartimento di Ingegneria, University of Campania "L. Vanvitelli", 81031, Aversa, Italy, (email: {sajjad.miralizadehjalala, alberto.cavallo, antonio.russo1, francesco.tucci}@unicampania.it).*
** *Polytechnic of Bari, Dept. of Electrical and Information Engineering, Via Re David 200, 70125 Bari, Italy (e-mail: {s.miralizadehjala, f.tucci4}@phd.poliba.it).*
*** *Dipartimento di Ingegneria Gestionale, dell'Informazione e della Produzione, Università degli Studi di Bergamo, 24044 Dalmine, Bergamo, Italy, (email: { antonio.russo}@unibg.it).*

Abstract: Faults are the primary cause of economic losses, equipment damage, and blackouts in distribution networks. These faults are categorized into various types and induce rapid fluctuations in voltage and current signals. In this paper, a machine learning-based fault detection method is considered. The proposed methodology effectively addresses the challenges of identifying fault types and locations in distribution power systems. By applying the Wavelet Packet Transform feature extraction method to superimposed three-phase voltage signals, the approach achieves high accuracy and robustness, even under noisy conditions and varying disturbances. The uncertainties associated with Renewable Energy Sources are considered, and the optimal locations of Monitoring Units are determined using a Voltage Stability Index-based optimization framework. Simulation results on a detailed IEEE 33-bus network validate the method's reliability, demonstrating its potential to enhance the efficiency and resilience of modern distribution networks.

Keywords: Fault Detection, Supervision, and Safety, Intelligent Control in Smart Grid, Smart Grids, Distributed and Decentralized Control and Management, Decision Support Systems.

1. INTRODUCTION

The optimal operation of distribution networks (DNs) is consistently threatened by various internal faults (e.g., malfunctioning electrical components, miscalculations) and environmental incidents (e.g., storms, lightning, etc.). According to Grainger and William (1994), these faults are either temporary or permanent. Conventional protection systems and devices can typically clear temporary faults. In contrast, permanent faults cannot be resolved remotely, and the deployment of maintenance crews is necessary. Furthermore, the expanded geographical coverage of DNs, their connection to sensitive loads and customers, the presence of extensive electrical equipment, and the high penetration of Renewable Energy Sources (RESs) introduce additional operational challenges to DNs.

Overvoltage, a primary characteristic of faults, occurs when the voltage amplitude exceeds the system's basic insulation level. While overvoltages typically do not cause immediate, substantial damage to DNs, undetected and unmitigated occurrences can escalate, leading to system-wide blackouts and posing stability concerns. These issues highlight the critical importance of effective fault detection and location in DNs.

Faults that induce overvoltages in DNs exhibit distinct characteristics and are typically classified into the following categories: single-phase-to-ground (LG), double-phase (LL), double-phase-to-ground (LLG), and three-phase-to-ground (LLLG) faults (see James et al. (2017)). Symmetrical faults, such as lightning strikes and LLLG faults, allow for balanced system modeling of DNs. In contrast, asymmetrical faults, including LG, LL, and LLG types, introduce phase imbalances, leading to unbalanced operating conditions, as described in Grainger and William (1994).

⋆ This work was partially funded by the European Union under GA no 101101961 - HECATE. Views and opinions expressed are however those of the author(s) only and do not necessarily reflect those of the European Union or Clean Aviation Joint Undertaking. Neither the European Union nor the granting authority can be held responsible for them. The project is supported by the Clean Aviation Joint Undertaking and its Members. Project co-funded by the European Union – Next Generation Eu - under the National Recovery and Resilience Plan (NRRP), Mission 4 Component 1 Investment 4.1 - Decree No. 118 (2nd March 2023) of Italian Ministry of University and Research - Concession Decree No. 2333 (22nd December 2023) of the Italian Ministry of University and Research, Project code D93C23000470005, within the Italian National Program PhD Programme in Autonomous Systems (DAuSy).

10.1016/j.ifacol.2025.08.110

The identification and detection of faults causing overvoltages in DNs attracts significant attention in the literature. Fault detection is essential in DNs' control and operation (Bansal and Sodhi (2018)) due to the direct connection of DNs to sensitive loads and components, as it enables rapid fault isolation and system recovery, thereby enhancing the reliability and stability of DNs. However, the complexity of DNs, their extensive geographical coverage, the lack of accurate network data, numerous consumers, the presence of RESs, and the high cost of certain equipment pose significant challenges to traditional fault detection methods. Recent advancements in measurement and communication technologies have enabled the development of hybrid approaches that integrate signal processing with machine learning (ML) techniques, as demonstrated in Peng et al. (2020). These approaches have gained considerable attention from researchers in recent years, offering promising solutions to enhance the accuracy and efficiency of fault detection and location in modern power systems.

On the other hand, ensuring precise and reliable data collection is a critical challenge in DNs due to the presence of numerous busbars and the sensitivity of ML-based methods to data accuracy and quality. Data reliability depends not only on the methods and equipment used for acquisition but also significantly on the placement of Monitoring Units (MUs). While some DNs are fully observable—meaning each busbar can serve as an MU—observability alone is not a sufficient criterion for determining the number and placement of MUs, as it overlooks efficiency and performance considerations. Originally rooted in control theory, the concept of observability has recently been extended to various fields, including cloud computing (Marie-Magdelaine et al. (2019), Costa et al. (2022)). Several studies have explored the observability of DNs through voltage measurements, such as Avendaño-Mora and Milanovic (2012). However, to address the limitations of observability-based approaches, numerous studies have proposed optimization methods for the placement of MUs and protection devices to improve fault detection performance (see Netto et al. (2022))

The Voltage Stability Index (VSI) is a key factor in determining the optimal placement of MUs. Various types of VSI exist, but this work employs the L-index (see Kessel and Glavitsch (1986)), a widely used metric for assessing power system stability. A comprehensive review of VSI methodologies is provided by Salama and Vokony (2022). In this study, an optimization problem is formulated using VSI as a criterion, along with the distance between MUs, to determine their optimal locations. As a result, the placement of MUs is strategically selected based on the VSI values.

Following the optimal placement of MUs, a hybrid approach is employed, combining signal processing and an ML-based method for fault type detection and location. Wavelet Packet Transform (WPT) is a powerful tool used to extract detailed coefficients, facilitating effective feature extraction. For instance, James et al. (2017) utilizes WPT and Deep Neural Networks (DNNs) to detect fault types and locations in DNs, though the fault location in that study is restricted to identifying positions within specific distances along four predefined lines in the grid. Additionally, Ray and Mishra (2016) presents a hybrid technique that combines WPT with Support Vector Machine (SVM) for fault detection and localization in DNs. A comprehensive review of fault monitoring, detection, and classification methodologies in power systems is presented by Labrador Rivas and Abrão (2020).

In this paper, a signal processing and ML-based approach is proposed to detect the type and location of faults in DNs. To mitigate the influence of noise and load variations, the superimposed fault voltage signal is utilized. Additionally, an optimization technique based on the VSI is proposed to determine the optimal placement of MUs. The WPT and other feature extraction techniques are employed to extract features from the voltage signals. The extracted data is then used in the fault detection process, where an NN-based classification method identifies different types of faults. Next, a fault location detection algorithm is proposed to accurately identify the precise location of the fault (i.e., the faulty busbar). In Hu et al. (2022), classification is carried out using data from all busbars, while this paper aims to achieve good results by using the minimum number of MUs.

2. PRELIMINARIES & PROBLEM FORMULATION

A three-phase AC DN is considered in this paper, consisting of a main voltage source, multiple RESs (such as photovoltaic systems and wind turbines) and n buses. The topology of the overall AC power network can be modeled as a connected, undirected graph $\mathcal{G} = (\mathcal{B}, \mathcal{E})$, where the nodes $\mathcal{B} = \{1, \ldots, n\}$ represent the buses, and the edges $\mathcal{E} = \{1, \ldots, p\}$ represent the power line interconnecting the buses. The bus nodes are divided into two sets, $\mathcal{B}_l$ and $\mathcal{B}_g$, representing the set of buses of consumers and generators, respectively, with $\mathcal{B}_l \cup \mathcal{B}_g = \mathcal{B}$. The DN is equipped with m voltage signals monitoring units MUs (referred to as monitors), where $m \leq n$ is large enough so that the observability property, intended as in Liao (2009), is guaranteed. Subsequently, the primary objective of this work can be stated as follows.

Objective 1. Given the AC DN represented by $\mathcal{G}$, equipped with m monitors, detect both the type and location of faults occurring within the network.

Objective 1 is achieved through a data-driven approach. By leveraging the data collected from the monitors, we aim to accomplish the following:

i) identifying different types of faults occurring within the DN,
ii) identifying the faulty busbar in the DN.

As outlined in the following sections, Objective 1 is addressed by developing data-driven algorithms, trained on data measured by the MUs (possibly in real-time).

Fault-type classification is a relatively straightforward task and can be accomplished using data from a single monitor. However, identifying faulty busbars is more complex and requires data from multiple monitors to achieve reliable performance. Additionally, incorporating multiple monitors enhances the robustness of fault-type classification, ensuring greater accuracy and reliability. Additionally, the optimal placement of MUs can significantly enhance system performance. Consequently, the strategic selection of

MU locations is critical to the effectiveness of the proposed fault detection and localization method. Moreover, the presence of measurement noise necessitates a robust approach to ensure accurate fault classification and precise fault location.

Thus, the secondary objective of this paper is formulated as follows.

Objective 2. Given the AC DN topology described by $\mathcal{G}$, equipped with m monitors, determine the optimal locations of the monitors that maximizes the fault type and fault location detection accuracy.

It is important to note that Objective 2 can be formulated as an optimization problem, whose solution is highly dependent on the DN's topology and the characteristics of the busbars. Solutions to this problem, focusing on observability, have been explored by Avendaño-Mora and Milanović (2012) using a mixed-integer linear programming approach.

3. OPTIMIZED MONITOR PLACEMENT IN DN

To achieve Objective 2, an optimization problem is formulated based on the VSI, with a prescribed minimum distance between monitors as a constraint. Among the possible VSIs proposed in the literature (see Kessel and Glavitsch (1986)), in this work, we adopt the so-called L-index. To define the L-index, for a given DN with n busbars, l loads and $n-l$ generators, let us indicate with $Y \in \mathbb{R}^{n\times n}$ the admittance matrix. The relationship between bus voltages and current injections is expressed as follows

$$\begin{bmatrix}\mathcal{I}_L\\ \mathcal{I}_G\end{bmatrix} = \begin{bmatrix}Y_{LL} & Y_{LG}\\ Y_{GL} & Y_{GG}\end{bmatrix}\begin{bmatrix}\mathcal{V}_L\\ \mathcal{V}_G\end{bmatrix}, \tag{1}$$

where $\mathcal{I}_L \in \mathbb{R}^l$ and $\mathcal{I}_G \in \mathbb{R}^{n-l}$ represent the current injection phasors at the load and generator buses, respectively; $\mathcal{V}_L \in \mathbb{R}^l$ and $\mathcal{V}_G \in \mathbb{R}^{n-l}$ denote the corresponding voltage phasors. The submatrices Y_{LL}, Y_{LG}, Y_{GL}, and Y_{GG} characterize the coupling between the load and generator buses. Rearranging the expression to solve for the load bus voltages yields

$$\mathcal{V}_L = -Y_{LL}^{-1}Y_{LG}\mathcal{V}_G = -F\mathcal{V}_G \tag{2}$$

where the term $-Y_{LL}^{-1}Y_{LG}$ captures the influence of generator buses on load buses. The L-index for load bus j is defined as follows

$$L_j = \left|1 - \sum_{i\in\mathcal{B}_g} F_{ji}\frac{\|\mathcal{V}_i\|}{\|\mathcal{V}_j\|}\right|, \quad \forall j \in \mathcal{B}_l, \tag{3}$$

where F_{ji} represents the element of the F matrix corresponding to load bus j and generator bus i. The L-index ranges from 0 (indicating complete stability) to 1 (indicating voltage collapse). Buses with higher L-index values are more susceptible to instability. Therefore, high values of L-index for a given busbar suggest the placement of a monitoring system at those busbars. Additionally, it is important to avoid clustering monitors in a single area. Thus, the monitor placement challenge can be framed as an optimization problem that balances two key objectives: positioning monitors at buses with high L-index values and maximizing their geographical dispersion. The goal is to select m buses from the set $\{1,\dots,n\}$ to maximize the Euclidean distances between them while ensuring optimal L-index coverage. This optimization problem can be formulated as follows

$$\max_{\omega}\ \frac{1}{\rho_1}L^\top\omega + \frac{1}{2}\frac{\gamma}{\rho_2}\left(\omega^\top \mathrm{D}\omega\right) \tag{4a}$$

$$\text{s.t.}\ \ \omega_i \in \{0,1\},\ \ \forall i \in \mathcal{B}_l, \tag{4b}$$

$$\omega_i = 0,\ \ \forall i \in \mathcal{B}_g, \tag{4c}$$

$$\sum_{i\in\mathcal{B}_l}\omega_i = m, \tag{4d}$$

$$\omega_i \mathrm{D}_{ij}\omega_j \geq \eta,\ \ \forall (i,j)\in\mathcal{B}_l\times\mathcal{B}_l\colon \omega_i=\omega_j=1, i\neq j \tag{4e}$$

where ω_i are binary variables that represent whether a monitor is installed on the i th busbar, D_{ij} is defined as the number of edges between the bus the i^{th} and the j^{th} bus and gives a measure of the distance between them, γ is a positive weight, η is the minimum distance to enforce between the busbars equipped with monitors and ρ_1, ρ_2 are normalization factors defined as

$$\rho_1 = \max_i L_i, \quad \rho_2 = \max_{i,j} D_{ij}.$$

The cost function (4a) tries to maximize the summation of L-indices among the busbars equipped with monitors while maximizing the distance between MUs. Here, the $\frac{1}{2}$ term is considered to avoid counting twice the distances D_{ij} and D_{ji}. Condition (4b) enforces the binary constraint for ω_i, while (4d) guarantees that the number of selected monitors will be equal to m. Finally, the minimum distance among monitors is guaranteed by (4e). The optimization problem (4) is a mixed-integer quadratic programming (MIQP) problem and can be solved by appropriate Disciplined Convex Programming (see Grant et al. (2006)) solvers. MIQP is the problem of optimizing a quadratic function over points in a polyhedral set where some of the components are restricted to be integral, Pia et al. (2017).

4. FAULT TYPE DETECTION DATA-BASED ALGORITHM

This section describes the proposed methodology to address the problem of fault location and classification based on ML. Firstly, it is essential to select a signal that effectively captures the most relevant features of the phenomenon while minimizing the impact of dynamic changes in the distribution network, such as harmonic ripple frequencies (HRF), load variations, and noise. In this context, superimposed voltage signals are employed as a robust solution. Some studies, such as Mishra and Deoghare (2014), propose fault detection methods based solely on WPT coefficients by comparing the energy levels of the coefficients in each phase before and after the fault. Specifically, the phases with the highest energy values can be identified as the faulty phases. However, these methods have poor performances in distinguishing between LL and LLG faults due to the similarity in their energy profiles. Therefore, we selected appropriate fault features and employed a neural network-based classification method to detect different types of faults and their locations accurately. The complete procedure presented in this paper is summarized in Fig. 1.

4.1 Feature Selection and Extraction

After identifying the optimal monitor locations, the superimposed voltage signals are computed to extract the

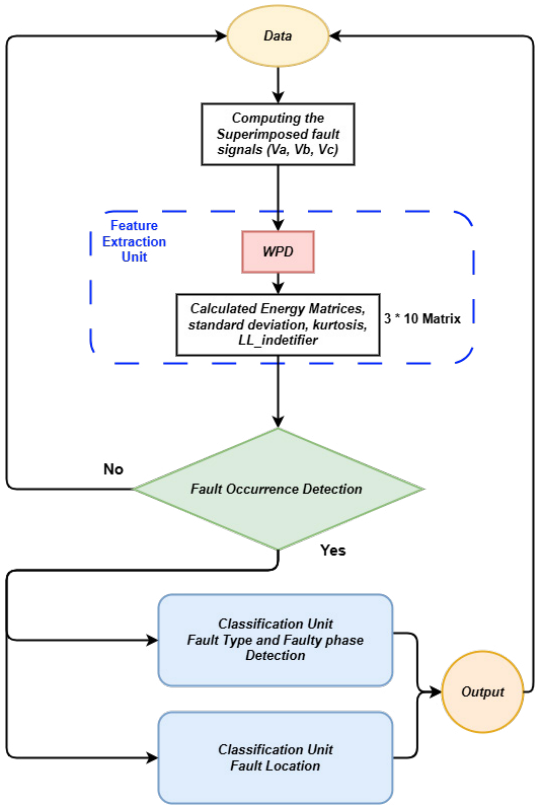

Fig. 1. Flowchart of the proposed fault type and location detection methodology

transient (non-periodic) components of the signal while eliminating the periodic components, including the fundamental frequency and the third and fifth harmonic signals (see (Isermann, 2006, Section 8)). Let $x(k)$ denote the k-th sample of the periodic voltage signal with p samples of x in a single period. Then, the transient faulty signal $\Delta x(k)$ can be computed as

$$\Delta x(k) = x(k) - x(k-p) \tag{5}$$

Note that, in the case of noisy measurement, it is possible to subtract a filtered version (e.g., by using a moving average FIR) of $x(k-p)$ in the above equation.

Using the computed transient faulty signal Δx, the next step is to select appropriate features for the machine learning process. Utilizing time-domain signals is not an efficient choice for data analysis due to large data storage requirements and high computational costs. Therefore, feature extraction methods are a crucial component of ML-based approaches. The WPT is one of the common feature extraction tools. In WPT, signals are decomposed into two components: detail coefficients $d_j(k)$, and approximation coefficients $a_j(k)$, (see Hess-Nielsen and Wickerhauser (1996)), as follows

$$f(t) = \sum_k \big(a_j(k)\phi(2^j t - b)\big) + \sum_j \sum_k d_j(k)\psi(2^j t - b), \tag{6}$$

where $\phi(w)$, and $\psi(w)$ represent the scaling and wavelet functions, respectively, which vary in type and shape. The approximations and details of the signal can be obtained as follows

$$a_j(k) = 2^j \int f(t)\phi(2^j t - k)dt \tag{7}$$

$$d_j(k) = 2^j \int f(t)\psi(2^j t - k)dt \tag{8}$$

where j and k represent the levels and coefficients of the WPT, respectively. In this paper, WPT with Daubechies 4 (db4) wavelet function is utilized.

A crucial aspect of applying the WPT method is the selection of appropriate coefficients. Various approaches for coefficient selection have been proposed in the literature. For example, coefficients can be chosen from a specific level of the WPT or selected to cover particular frequency intervals commonly observed in fault signals. Indicating with $s_{i-j}(t)$ the selected coefficients of the WPT, with i and j denoting the levels and scales of the WPT coefficient, respectively, their energy can be calculated using the following equations for discrete signals

$$E_{i-j} = \sum_{-\infty}^{+\infty} |s_{i-j}(t)|^2. \tag{9}$$

In this paper, we utilize the coefficients derived from the methodology established in Miralizadeh Jalalat et al. (2023) and subsequently calculate their energy. A list of the coefficients' energies corresponding to each phase (here, phase A) obtained using (9) is presented as follows

$$E_A = [E_{10-1}, E_{11-3}, E_{11-1}, E_{8-1}, E_{9-3}, E_{8-3}, \ldots E_{10-6}, E_{11-13}, E_{9-6}, E_{9-1}]. \tag{10}$$

Finally, these coefficients are summed across the three phases and considered as *the first three elements* of the feature matrix. Six additional features are computed by evaluating the standard deviations and kurtosis for each phase of the superimposed signals, where the kurtosis operator for a signal s is defined as

$$\kappa[s] = \mathbb{E}\left[\left(\frac{s-\mu}{\sigma}\right)^4\right] = \frac{\mu_4}{\sigma^4}, \tag{11}$$

where μ_4 is the fourth central moment and σ is the standard deviation of s. This results in nine computed features. Furthermore, to distinguish between LL and LLG faults, one more feature is considered, namely, the zero-sequence voltage of the faulty phase, calculated as the summation of the voltages of the three phases. For LL faults, this value is zero, while for other faults, it is assigned a value of 1 (see Grainger and William (1994)). Such an additional feature is defined as

$$\zeta = \begin{cases} 0 \text{ if } (V_a + V_b + V_c) = 0 \\ 1 \text{ othervwise} \end{cases} \tag{12}$$

Finally, the vector of selected features for a single fault is given by

$$\Xi = [E_A, E_B, E_C, \sigma_A, \sigma_B, \sigma_C, \kappa_A, \kappa_B, \kappa_C, \zeta] \tag{13}$$

4.2 Machine Learning-Based Fault Detection algorithm

After selecting and extracting the features, the next step is to choose an appropriate method for fault detection and location. This paper considers ten different types of faults, and a classification technique is employed to identify and locate them accurately.

In this paper, fault classification is performed using neural networks, in particular, a fully connected Feedforward

Neural Network (FFNN), a powerful machine learning approach well suited for handling complex and high-dimensional data. The neural network architecture comprises an input layer, multiple hidden layers, and an output layer, enabling it to capture intricate patterns and relationships within the data. The input layer receives the feature vector, as defined in (13). Each hidden layer processes its inputs by computing a weighted sum, followed by applying an activation function. For the j^{th} neuron in the l^{th} layer, the output $z_j^{(l)}$ is given by

$$z_j^{(l)} = \sum_{i=1}^{q} w_{ji}^{(l)} a_i^{(l-1)} + b_j^{(l)} \tag{14}$$

where $w_{ji}^{(l)}$ is the weight connecting the i-th neuron in the $(l-1)^{th}$ layer to the j^{th} neuron in the l^{th} layer, $a_i^{(l-1)}$ is the activation of the i^{th} neuron in the $(l-1)^{th}$ layer, $b_j^{(l)}$ is the bias term, and q represents the number of neurons. Commonly used activation functions are ReLU, hyperbolic tangent, and sigmoid functions, adopted in this work and defined as

$$a_{\text{out}} = \sigma(z_{\text{out}}) = \frac{1}{1+e^{-z_{\text{out}}}}. \tag{15}$$

The output a_{out} represents the probability of the positive class. The loss function measures the difference between the predicted probabilities and the true labels. For binary classification, the binary cross-entropy loss is commonly used

$$\mathcal{L} = -\frac{1}{N}\sum_{i=1}^{N}\left[y_i \log(a_{\text{out}}^{(i)}) + (1-y_i)\log(1-a_{\text{out}}^{(i)})\right], \tag{16}$$

where y_i is the true label (0 or 1) for the i^{th} instance, and $a_{\text{out}}^{(i)}$ is the predicted probability.

5. NUMERICAL RESULTS

The IEEE 33-bus standard network is selected to evaluate the proposed method. To analyze the impact of RESs, three types of RESs are integrated into buses 6, 15, and 30 of the network. Table 1 presents the specifications of the RESs, including their initial power values, along with the mean and standard deviation used to model RES uncertainties.

Table 1. Specifications of the RESs

DN	Locations	Mean power (p.u.)	STD power (p.u.)
IEEE 33	6, 15, 30	0.2, 0.15, 0.1	0.05, 0.03, 0.02

The optimization problem (4), which accounts for the locations of the RESs, has been solved. The MU locations are determined to be buses 18, 25, and 33. The results obtained from the proposed approach are compared with those from the study by Hu et al. (2022), which employs an MU at every busbar of the IEEE 33-bus network. Hu et al. (2022) employs deep graph learning for fault diagnosis and utilizes a specialized spatiotemporal convolutional block to extract features from voltage waveforms. The presence of RESs, load variations, and noise effect is taken into account in Hu et al. (2022). These phenomena are also considered in our paper.

The use of a limited number of monitors placed in optimal locations, along with the utilization of voltage superimposed signals from the MUs to eliminate additional harmonic signals and mitigate the impact of non-periodic noise in MU measurements, represents some of the key differences between this study and Hu et al. (2022).

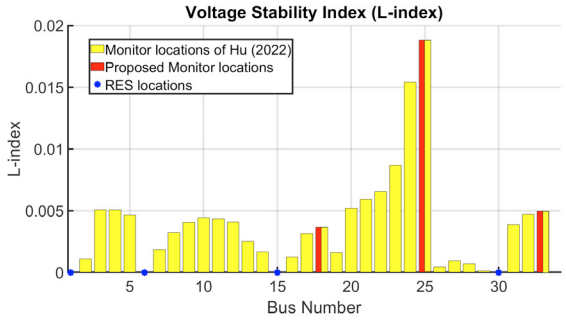

Fig. 2. L-Index of the IEEE 33-bus system showing the locations of RESs and monitoring units

It should be noted that Hu et al. (2022) employs two classifiers: one for fault detection and another for fault location identification, including the distinction of faults occurring between two adjacent MUs. Similarly, this study utilizes two classification methods for fault detection and fault location identification.

Fig. 2 shows the L-indices for selected busbars in the IEEE 33-bus network. The busbars highlighted in red indicate the monitor locations proposed in this study, while those marked in yellow correspond to the locations suggested in Hu et al. (2022). Additionally, Table 2 summarizes the dataset specifications.

After selecting the optimal monitor locations, simulations are conducted on the case studies to collect data and apply the proposed approach for fault type and location detection. For comparison, the results of the proposed approach using the selected monitor locations are evaluated against those of the Hu et al. (2022) study. Moreover, the specifications of the FFNN employed for fault detection and location are summarized in Table 3.

The classification results are summarized in Table 4. As shown in this table, the fault type detection component of the proposed method remains accurate even when data from one of the monitors is unavailable. This demonstrates the robustness of the approach, as it maintains high accuracy despite the lack of information from one or even two monitors. To highlight the efficiency of optimizing the location of the MU in the accuracy of the results, three randomly selected buses - 6, 21, and 33 - are equipped with MU for comparison with the proposed locations of the MU.

The results of the fault location analysis are presented in Table 5, illustrating the accuracy of fault location. While the proposed method demonstrates reliable fault detection, the fault location accuracy is comparatively less

Table 2. Specifications of the data

Considered fault types	LG, LL, LLG, LLLG
Total number of simulations	27720
Variations	Fault time, resistance, faulty phase
Size of train data	19404
Size of test data	8316

Table 3. Specifications of the Neural Network

Number of Layers	2
Number of Neurons in each layer	212, 287
Activation Function	Sigmoid

robust and requires further investigation in future studies. Specifically, utilizing data from all monitors is crucial to achieving accurate fault location results.

Table 4. Fault type detection results accuracy in the IEEE 33-bus network

Monitor location	Training Accuracy	Testing Accuracy
(18, 25, 33)	99.8%	99.9%
(6, 21, 33)	99.5%	99.7%
18	99.5%	99.68%
25	98.9%	99.3%
33	99.4%	99.4%
Hu et al. (2022)	**	98%

6. CONCLUSION

This study presents a robust machine learning-based approach to fault detection and location in DNs, effectively addressing the challenges posed by various types of faults and their impact on voltage signals. By leveraging WPT analysis of superimposed voltage signals and optimizing MU placement through a VSI-based framework, the proposed method achieves high accuracy and resilience, even in the presence of noise and uncertainties associated with RESs. Validation on the IEEE 33-bus network demonstrates the approach's reliability and practical applicability. These findings underscore the potential of the proposed method to enhance operational efficiency, fault management.

REFERENCES

Avendaño-Mora, M. and Milanovic, J.V. (2012). Monitor placement for reliable estimation of voltage sags in power networks. *IEEE Transactions on Power Delivery*, 27(2), 936–944.

Avendaño-Mora, M. and Milanović, J. (2012). Generalized formulation of the optimal monitor placement problem for fault location. *Electric Power Systems Research*, 93, 120–126.

Bansal, Y. and Sodhi, R. (2018). Microgrid fault detection methods: Reviews, issues and future trends. In *2018 IEEE Innovative Smart Grid Technologies - Asia (ISGT Asia)*, 401–406.

Costa, B., Bachiega, J., Carvalho, L.R., Rosa, M., and Araujo, A. (2022). Monitoring fog computing: A review, taxonomy and open challenges. *Computer Networks*, 215, 109189.

Table 5. Fault location outcomes accuracy in the IEEE 33-bus network

Monitor/(s) location	Training Accuracy	Testing Accuracy
(18, 25, 33)	95.2%	96.7%
(6, 21, 33)	94.8%	95.1%
18	52.1%	55.8%
25	50.2%	50.6%
33	61.6%	67.2%
Hu et al. (2022)	**	98%

Grainger, J.J. and William, D.S. (1994). *Power System Analysis*. McGraw-Hill, 1994.

Grant, M., Boyd, S., and Ye, Y. (2006). *Disciplined Convex Programming*, 155–210. Springer US, Boston, MA.

Hess-Nielsen, N. and Wickerhauser, M.V. (1996). Wavelets and time-frequency analysis. *Proceedings of the IEEE*, 84(4), 523–540.

Hu, J., Hu, W., Chen, J., Cao, D., Zhang, Z., Liu, Z., Chen, Z., and Blaabjerg, F. (2022). Fault location and classification for distribution systems based on deep graph learning methods. *Journal of Modern Power Systems and Clean Energy*, 11(1), 35–51.

Isermann, R. (2006). *Fault-Diagnosis Systems: An Introduction from Fault Detection to Fault Tolerance*. Springer Berlin Heidelberg.

James, J., Hou, Y., Lam, A.Y., and Li, V.O. (2017). Intelligent fault detection scheme for microgrids with wavelet-based deep neural networks. *IEEE Transactions on Smart Grid*, 10(2), 1694–1703.

Kessel, P. and Glavitsch, H. (1986). Estimating the voltage stability of a power system. *IEEE Transactions on Power Delivery*, 1(3), 346–354.

Labrador Rivas, A.E. and Abrão, T. (2020). Faults in smart grid systems: Monitoring, detection and classification. *Electric Power Systems Research*, 189, 106602.

Liao, Y. (2009). Fault location observability analysis and optimal meter placement based on voltage measurements. *Electric Power Systems Research*, 79(7), 1062–1068.

Marie-Magdelaine, N., Ahmed, T., and Astruc-Amato, G. (2019). Demonstration of an observability framework for cloud native microservices. In *2019 IFIP/IEEE Symposium on Integrated Network and Service Management, IM 2019*, 722 – 724.

Miralizadeh Jalalat, S., Miralizadeh, S., Talavat, V., and Boalndi, T.G. (2023). A novel superimposed voltage energy-based approach for single phase to ground fault detection and location in distribution networks. *IET Generation, Transmission & Distribution*, 17(18), 4215–4233.

Mishra, R.C. and Deoghare, P.M. (2014). Analysis of transmission line fault by using wavelet. *International journal of engineering research and technology*, 3.

Netto, M., Krishnan, V., Zhang, Y., and Mili, L. (2022). Measurement placement in electric power transmission and distribution grids: Review of concepts, methods, and research needs. *IET Generation, Transmission & Distribution*, 16(5), 805–838.

Peng, N., Liang, R., Wang, G., Sun, P., Chen, C., and Hou, T. (2020). Edge computing-based fault location in distribution networks by using asynchronous transient amplitudes at limited nodes. *IEEE Transactions on Smart Grid*, 12(1), 574–588.

Pia, A.D., Dey, S.S., and Molinaro, M. (2017). Mixed-integer quadratic programming is in np. *Mathematical Programming*, 162, 225–240.

Ray, P. and Mishra, D.P. (2016). Support vector machine based fault classification and location of a long transmission line. *Engineering science and technology, an international journal*, 19(3), 1368–1380.

Salama, H.S. and Vokony, I. (2022). Voltage stability indices–a comparison and a review. *Computers & Electrical Engineering*, 98, 107743.